Rotational IMRT delivery using a digital linear accelerator in very high dose rate 'burst mode'

2011 Phys. Med. Biol. 56 1931

(http://iopscience.iop.org/0031-9155/56/7/002)

Phys. Med. Biol. **56** (2011) 1931–1946 doi:10.1088/0031-9155/56/7/002

Rotational IMRT delivery using a digital linear accelerator in very high dose rate 'burst mode'

Bill J Salter[1], Vikren Sarkar[1], Brian Wang[1], Himanshu Shukla[2], Martin Szegedi[1] and Prema Rassiah-Szegedi[1]

[1] Department of Radiation Oncology, University of Utah, Salt Lake City, UT, USA
[2] Oncology Care Systems Group, Siemens Medical Solutions (USA), 4040 Nelson Avenue, Concord, CA, USA

E-mail: bill.salter@hci.utah.edu

Received 25 December 2010, in final form 7 February 2011
Published 2 March 2011
Online at stacks.iop.org/PMB/56/1931

Abstract

Recently, there has been a resurgence of interest in *arc-based* IMRT, through the use of 'conventional' multileaf collimator (MLC) systems that can treat large tumor volumes in a single, or very few pass(es) of the gantry. Here we present a novel 'burst mode' modulated arc delivery approach, wherein 2000 monitor units per minute (MU min^{-1}) high dose rate bursts of dose are facilitated by a flattening-filter-free treatment beam on a Siemens Artiste (Oncology Care Systems, Siemens Medical Solutions, Concord, CA, USA) digital linear accelerator in a non-clinical configuration. Burst mode delivery differs from continuous mode delivery, used by Elekta's VMAT (Elekta Ltd, Crawley, UK) and Varian's RapidArc (Varian Medical Systems, Palo Alto, CA, USA) implementations, in that dose is not delivered while MLC leaves are moving. Instead, dose is delivered in bursts over very short arc angles and only after an MLC segment shape has been completely formed and verified by the controller. The new system was confirmed to be capable of delivering a wide array of clinically relevant treatment plans, without machine fault or other delivery anomalies. Dosimetric accuracy of the modulated arc platform, as well as the Prowess (Prowess Inc., Concord, CA, USA) prototype treatment planning version utilized here, was quantified and confirmed, and delivery times were measured as significantly brief, even with large hypofractionated doses. The burst mode modulated arc approach evaluated here appears to represent a capable, accurate and efficient delivery approach.

(Some figures in this article are in colour only in the electronic version)

1. Introduction

Since the advent of intensity modulated radiotherapy (IMRT) in the mid-1990s, there has been steadily growing demand for extremely conformal isodose distributions for use in radiation therapy. Recently, there has been a resurgence of interest in *arc-based* IMRT, through the use of 'conventional' multileaf collimator (MLC) systems that can treat large tumor volumes in a single, or very few pass(es) of the gantry (Li *et al* 2001, Otto 2008, Yu 1995), with commercial systems including Elekta's system VMAT (Bedford 2009, Bedford and Warrington 2009, Haga *et al* 2009) (Elekta Limited, Crawley, UK) and Varian's RapidArc system (Kjaer-Kristoffersen *et al* 2009, Ling *et al* 2008, Mayo *et al* 2009, Zacarias *et al* 2009) (Varian Oncology, Palo Alto, CA, USA). Such interest has been driven in large part by a desire to achieve the plan quality afforded by many-field static gantry approaches, (e.g. 5–9 IMRT fields) while simultaneously reducing the significant amount of time that is typically required to deliver such high quality treatment plans. Through a combination of the power and degrees of freedom of intensity modulation with the added power and spatial degrees of freedom afforded by an arc-based delivery approach, this goal of very high plan quality combined with extremely efficient delivery is proving to be achievable in many cases.

In parallel with such work, other groups have been investigating the characteristics of a flattening-filter-free linear accelerator (Ponisch *et al* 2006, Stathakis *et al* 2009). Because a flattening filter is known to introduce significant amounts of beam attenuation, with an associated significant decrease in output dose rate, multiple investigators have noted that removal of the flattening filter can lead to a large gain in the central-axis dose rate. If such dose rate improvements were compatibly coupled with the delivery efficiency of a modulated arc delivery approach, it would seem reasonable to assume that potentially significant improvements in delivery efficiency might be realized. We note that Bayouth *et al* have previously reported on performance characteristics of an Oncor model linac (Oncology Care Systems, Siemens Medical Solutions, Concord, CA, USA) operated at 1000 MU min^{-1} by removal of the flattening filter, for cone-based stereotactic treatments (Bayouth *et al* 2007). Additionally, Siemens (Oncology Care Systems, Concord, CA, USA) has recently released a fully digital *Artiste* linear accelerator that includes a new 160-leaf MLC (Bayouth 2008, Tacke *et al* 2008) which offers a combination of high leaf-motion speeds (4 cm s^{-1}), very low leaf transmission values of approximately 0.4% (Tacke *et al* 2008) and a leaf span of 20 cm. The linac is fully digital and, when converted with software and firmware into a testing mode, is capable of producing extremely high dose rate, flattening-filter-free photon beams. Furthermore, because of the digital nature of the Artiste platform, the linac can be configured to be capable of delivering high dose rate *bursts* of dose at discrete, well-defined gantry angles, which can very closely approach the method by which arc-based IMRT deliveries are typically modeled for treatment planning calculation (i.e. as a summation of discrete, statically delivered segments).

In this work we test modifications that allow the linac to perform modulated arc delivery using a very high dose rate of 2000 MU min^{-1} with a flattening-filter-free beam operated in so-called 'burst mode'. To support the creation of burst mode treatment plans that the linear accelerator can deliver, a prototype version of a commercial treatment planning system (TPS) is also tested.

The purpose of this work is twofold. First, we perform proof of principle testing for burst mode delivery using the Artiste. We assess the ability of the linac to successfully deliver such high dose rate, modulated arc plans for multiple, clinically relevant disease sites, and we also assess the efficiency of the delivery method relative to other standard delivery approaches. Secondly, by performing rigorous dose quality assurance on these treatment plans, we test

the ability of the linac to accurately deliver and the prototype TPS to accurately predict, the dose distributions that result from the linac being operated in burst mode for modulated arc delivery.

2. Materials and methods

2.1. Burst mode delivery briefly described

For purposes of understanding burst mode, it should first be contrasted with the more familiar continuous delivery mode utilized by commercially available modulated arc solutions from Varian Medical (Rapid Arc) and Elekta Oncology (VMAT).

During continuous mode delivery, MLC motion is performed simultaneously with dose delivery (i.e. beam on). This means that dose is being delivered while MLC segments are being reshaped, and that over any given window of dose delivery, the IMRT segment shapes must be interpolated between explicitly calculated shapes to ensure an achievable, continuous leaf configuration motion (see figure 1). In order to maximize dose delivery accuracy, continuous, high temporal and spatial resolution monitoring of leaf position is performed to ensure that errors in leaf position, as a function of time, are minimized (Feygelman *et al* 2010). Dose rate and gantry speed are both modulated to allow for delivery of the correct dose per IMRT segment and an MLC velocity servo is required to continuously adjust the leaf velocity to facilitate accurate, and timely, leaf positioning. For continuous mode delivery, continuous synchronization between leaf movement, gantry movement and dose rate is, therefore, required for accurate dose delivery.

Burst mode, as opposed to continuous mode, does not employ dose delivery that occurs at the same time as MLC leaf motion. Instead, MLC leaves are moved rapidly into position to establish the next IMRT segment shape that is to be delivered from a particular gantry angle, and then dose is delivered. Dose is only delivered once the leaf positions are verified to be accurate to within the stated tolerance of the MLC (0.5 mm for the Siemens 160 MLC) and there are no interpolated, or transitional, segment shapes at which dose is delivered. Such an approach has been previously used by the ERGO++ TPS (3D Line Medical Systems, Milan, Italy) as described by Yoda *et al* (2009).

Because of the very high 2000 MU min^{-1} dose rate that is available in burst mode, the MU/segment required for even very high dose protocols (e.g. stereotactic body radiation therapy—SBRT) can be delivered over a relatively small arc angle, referred to as α. This small dose delivery window can be chosen to be well centered on the desired segment angle, as shown in figure 2. It should be noted that, if a treatment plan is developed so that IMRT segments are to be delivered every 10°, a typical TPS will calculate total dose by simplifying the delivery scheme to assume that the arc-based treatment is delivered as 36 static fields, separated by 10° each. It is a unique feature of burst mode delivery that the treatment delivery will very closely approximate this TPS assumption (see figure 2).

Additionally, the modified controller firmware utilized at the linear accelerator (linac) is designed to automatically modulate gantry speed so that the angle over which dose is delivered, α, is minimized, or 'squeezed'. As an example, for situations where a very high dose is to be delivered for a particular segment, as might be required for SBRT, the gantry speed will be slowed down to ensure that α is still small. However, because the gantry speed can be modulated throughout the arc, other segments that do not require such high monitor units (MU) are not needlessly penalized by requiring that they also move at a slow gantry speed. By utilizing this approach, the delivery speed can be optimized to be as fast and efficient as possible, while still allowing for small α angle of dose delivery per delivered segment. Finally,

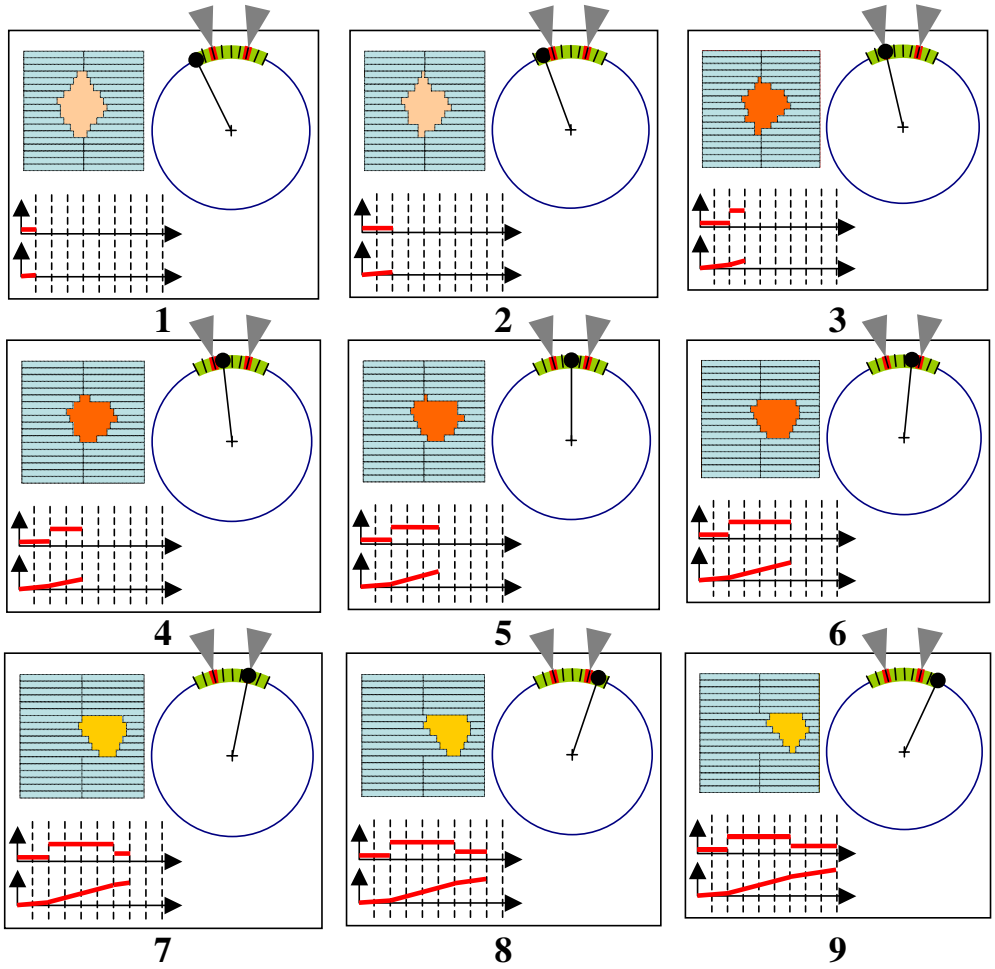

Figure 1. Example of continuous mode delivery. The gray pointers above the red hash marks indicate two angles at which segment shapes explicitly calculated by the treatment planning system are to be delivered. The green shaded hash marks indicate angles at which MLC leaves are transitioning from one explicit segment shape to another. Also shown are examples of MLC segment shapes, shaded according to dose that is being delivered. The orange shading for the MLC opening indicates highest dose level being delivered at explicitly calculated angles, with lower dose rates demonstrated for transitional segment shapes. Instantaneous and cumulative dose levels are also depicted in the lower left plot. The top graph shows the change of dose rate with time and the lower graph shows the accumulation of dose with time.

it should be noted that in order to ensure accurate MU linearity, the software linearly reduces the dose rate from the maximum of 2000 MU min^{-1} for segments with more than 10 MU to 500 MU min^{-1} for segments with 1 MU.

2.2. Machine conversion

As the treatment machine has not yet received regulatory clearance for clinical use of modulated arc in burst mode, the linac was converted into burst mode by use of a motor controller board

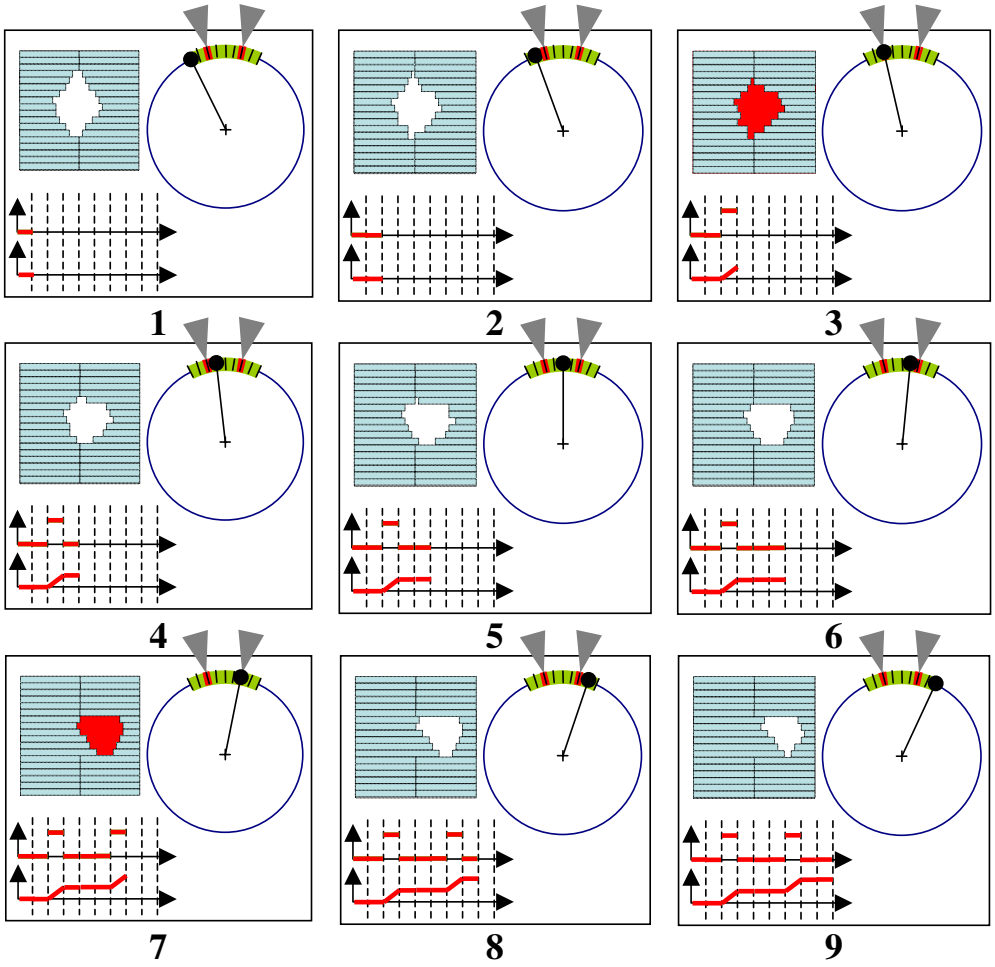

Figure 2. Example of burst mode. The gray pointers above the red hash marks indicate two angles at which segment shapes explicitly calculated by the treatment planning system are to be delivered. The green shaded hash marks indicate angles at which MLC leaves are transitioning from one explicit segment shape to another but, as opposed to continuous mode delivery, no dose is being delivered at these angles. The width of the red hash marks can be thought of as being indicative of the angle α over which dose is delivered. α can be made small due to the high dose rate delivery used in burst mode (i.e. 2000 MU min^{-1}) and due to strategic slowing of the gantry, as needed. Also shown are examples of MLC segment shapes, shaded according to dose that is being delivered. The red shading for the MLC opening indicates highest dose level being delivered at the explicitly calculated angles, with white shading indicating that no dose is being delivered at other angles. This is also depicted by the plots at the lower left showing instantaneous (top graph) and cumulative dose (lower graph) levels per angle.

with appropriately configured firmware. We note that all relevant software and hardware interlocks are maintained intact following conversion. This firmware then modulates the gantry speed, turns on the beam at the correct gantry positions, supervises the treatment through each α angle and handles various exceptions and error conditions. Once converted, the linac is capable of performing modulated arc burst mode deliveries using a flattening-filter-

free photon beam with a nominal energy of 6 MV and a dose rate of up to 2000 MU min^{-1}, as described in the previous section.

2.3. Prototype treatment planning system

A prototype version of the Prowess Panther TPS (v5.01, Prowess Inc., Concord, CA, USA) was used for the creation of numerous arc-based treatment plans. For purposes of context/comparison, treatment plans were also calculated and delivered for multiple other delivery approaches to include 3D conformal, static gantry IMRT, conformal arc and segment-weighted conformal arc. For modulated arc deliveries, in addition to being required to provide the starting and ending gantry positions for the arc, the user must provide the spacing between each optimization point (OP) about the arc. OPs consist of the angles at which the TPS is intended to develop optimized segment shapes, the segment shapes themselves and their associated weights, or MU. Associated with the optimization points is a quantity denoted as α in the TPS, and described previously in section 2.1. For the TPS, α represents the extent of the arc, centered about each OP, where beam delivery is allowed to occur. For example, if there is an OP specified to be at 320° with an α of 5° (the default value of α used for all plans developed here); this means that dose can be delivered from 317.5° to 322.5°. The numerical value of α is initially entered by the user into the TPS as, essentially, an upper limit to be placed on α. The planning system, equipped with an understanding of maximum and minimum gantry speeds and maximum dose rate for the specific linac, then develops a modulated arc plan that respects the maximum and minimum MU that can be delivered over the user-specified α angle. At the time of delivery the modified controller firmware at the linac (as discussed in the last paragraph of section 2.1) will intelligently vary gantry speed and beam on angle to ensure that α is never exceeded, and will reduce the angle α over which dose is delivered, if possible. The angle α is transmitted as part of the treatment plan to the treatment machine for use in delivery, but the actual TPS calculations are performed, as described previously, as if the entire dose is delivered in a static fashion, centered about the actual OP location. It should be noted that the value of α indirectly imposes a real-world minimum and maximum dose limit that can be delivered about that angle, as a function of gantry speed. For clinically relevant plans, the maximum dose per segment has not been approached, and the minimum dose of 1 MU per segment has not posed any measurable penalties on plan quality. For the Artiste configured in burst mode, the maximum MU/degree is 111 MU/degree and occurs at the minimum gantry speed of 0.3° s^{-1}. The maximum MU/degree while operating at the maximum gantry speed of 6° s^{-1} is 5.55 MU/degree. For single-pass arcs, the TPS allows for one MLC segment shape and weight per OP, and for multiple-pass arcs, multiple segment shapes and weights are developed, one for each pass stipulated. All treatment plans studied here were of the single pass variety.

The user also has the option to choose between three different types of arcs: (1) conformal arc (CA), (2) segmented-weighted conformal arc (SWCA) and (3) modulated arc (MA). For a conformal arc, the shape of the MLC conforms to the beam's eye view shape of the target for that particular gantry angle, or OP, and the beams are equally weighted for every port in the arc. For a segment-weighted arc, the shape of each segment is the same as in a conformal arc but the inverse planning system optimizes the weight of each port so as to best meet the inverse planning constraints. For a modulated arc, as described previously, the inverse planning system develops a single optimized segment shape and weight at each user specified OP. For delivery approaches which employ inverse planning (i.e. SG-IMRT, SWCA and MA) the TPS utilizes simulated annealing optimization (Kirkpatrick *et al* 1983) for beam optimization. Beam shapes and weights for the three different arc-based treatment types are

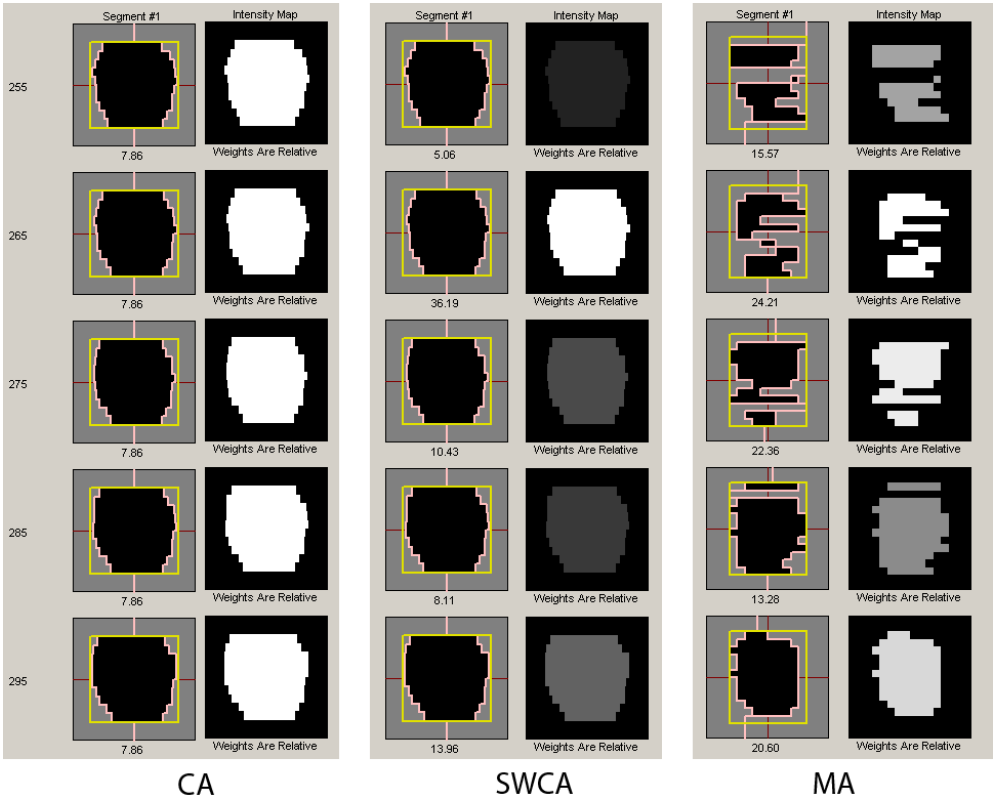

Figure 3. Depiction of the difference between conformal arcs (CA), segment-weighted conformal arcs (SWCA) and modulated arcs (MA) at five gantry angles. The numerical values in the segment column are MU, which are also proportionally shown in the intensity map column as gray shade.

shown in figure 3 for further clarification. It should be noted that all three arc modalities are delivered using the burst mode approach.

2.4. Plan creation and treatment sites

For this study, we deemed it important to investigate treatment plans for a wide array of clinically relevant sites. Therefore, treatment plans were created for each of the following sites: (a) cavernous sinus, (b) lung, (c) prostate, (d) liver, (e) spine and (f) head and neck.

To ensure relevance of the validation, and equivalence of plans, treatment plans followed the planning guidelines from relevant Radiation Therapy Oncology Group (RTOG) protocols, or the Radiological Physics Center (RPC) guidelines used during the credentialing process for protocol studies. If RTOG protocols were used, the plans were permitted to have minor deviations (as defined by the protocol) but major deviations were not allowed except for the CA and SWCA plans, where the limited degrees of freedom afforded by the respective approach might make it impossible to simultaneously satisfy all plan requirements. For a few sites where neither RTOG nor RPC guidelines were available, we used our internal department

Table 1. List of clinical sites investigated along with planning parameters used.

Treatment site	Prescription (Gy)	Number of fractions	Source of end-point criteria
Cavernous sinus SRS	15	1	Clinical case
Lung SBRT	60	3	RTOG 0618
Prostate	73.8	41	RTOG 0415
Prostate	70	28	RTOG 0415
Liver SBRT	36	3	Clinical case
Spine	6	1	RPC spine phantom
Head and neck	6.6	1	RPC head and neck phantom

planning guidelines. Table 1 lists the sites, prescription level, number of fractions and source of planning end-points used to create the plans for this project.

For the purposes of characterizing burst mode delivery accuracy, three plans were created for each of the eight sites listed in table 1: (1) a conformal arc plan, (2) a segment-weighted conformal arc plan and (3) a modulated arc plan. For all arc plans, a total of 36 OPs were used, equally spaced at 10° intervals over the whole arc, except for the liver plan where we used only a 220° arc (22 OPs) to specifically avoid the spinal cord. For all cases, the value of α was nominally set to 5°. Once a plan was created using an appropriately anonymized patient CT, the Prowess TPS was used to create a corresponding hybrid phantom plan by recalculating the dose distribution that would result on a phantom geometry for the same beam parameters. Once created, the hybrid plans were exported as DICOMRT objects for the delivery process. In addition to the 21 plans just described for dosimetric validation purposes, 14 additional treatment plans were also developed using 3D conformal and static gantry IMRT delivery approaches, for the purposes of collecting delivery time data for comparison with the arc-based methods. The total number of plans calculated and delivered, thus, totaled 35.

2.5. Plan delivery and data analysis

The DICOM-RT treatment plan object was transferred by file transfer to the laptop computer connected to the linac console. Plans were loaded and converted to the appropriate Siemens delivery format (DMIP: Digital Machine Interface Protocol) using a vendor-provided script on the laptop before being sent to the console.

Delivered dose was validated using a Delta4 (Bedford *et al* 2009) arc validation system (ScandiDos, Uppsala, Sweden). The Delta4 system consists of 1069 diode detectors located in two intersecting planes consisting of three separate panels with central detector spacing of 0.5 cm for the central 6 cm × 6 cm region and 1.0 cm spacing for the remainder of the detectors. The detectors are disks with 1 mm diameter and 0.1 mm thickness. The system is capable of measuring a volumetric representation of delivered dose and then comparing it to the volumetric dose calculated by the TPS to characterize the accuracy of the delivery. The manufacturer's recommended calibration protocol was followed to calibrate both intersecting planes (i.e. all three panels) of the device so that absolute dose measurement could be performed. For all validation runs, the Delta4 measurement device was accurately positioned to isocenter using the lasers in the vault and the plan was delivered to the unit. After delivery, the software provided with the system was used to analyze the delivered dose and provide the percentage of the 1069 discrete measurements that passed using a gamma criterion

Table 2. Summary of the dose validation results of all arc-based plans as measured on the Delta4 system. Mean% gamma agreement: CA = 98.8% ± 2.1%, SWCA = 98.2% ± 2.0%, MA = 98.1% ± 2.1%. Data show that the burst mode MA introduced here validates well, and in fact, as well as the other, simpler arc-based approaches of CA and SWCA.

Site	Modality	Rx dose (Gy)	Measured dose (Gy)	Expected dose (Gy)	CAX point dose difference (%)	Percentage gamma pass rate (3%, 3 mm)	Total MUs
Cavernous sinus	CA	15.0	16.15	16.32	−1.1%	94.6%	2656.1
	SWCA	15.0	15.93	16.12	−1.2%	95.4%	2625.4
	MA	15.0	14.90	15.02	−0.8%	96.1%	3659.1
Lung	CA	20.0	23.97	23.63	1.4%	100.0%	3827.9
	SWCA	20.0	23.41	23.13	1.2%	99.3%	3751.6
	MA	20.0	23.97	24.28	−1.3%	97.1%	4461.8
Prostate	CA	1.8	1.98	1.97	0.5%	100.0%	299.2
	SWCA	1.8	1.93	1.96	−1.6%	100.0%	295.2
	MA	1.8	1.83	1.83	0.0%	100.0%	317.3
Prostate	CA	2.5	2.75	2.74	0.4%	100.0%	415.6
	SWCA	2.5	2.70	2.73	−1.1%	100.0%	410.3
	MA	2.5	2.59	2.60	−0.4%	100.0%	430.8
Liver	CA	12.0	14.88	14.79	0.6%	97.3%	2283.4
	SWCA	12.0	15.70	15.62	0.5%	97.8%	2413.8
	MA	12.0	15.00	14.91	0.6%	95.1%	3225.0
Spine RPC phantom	CA	6.0	6.54	6.55	−0.2%	100.0%	994.2
	SWCA	6.0	6.28	6.38	−1.6%	95.6%	998.2
	MA	6.0	7.32	7.11	2.9%	100.0%	1717.6
H&N RPC phantom	CA	6.6	6.31	6.36	−0.8%	99.5%	968.4
	SWCA	6.6	6.45	6.42	0.5%	99.2%	945.6
	MA	6.6	5.69	5.79	−1.8%	98.7%	1293.1

of 3% and 3 mm. The daily temperature correction was used to account for a change in temperature from the time of calibration and linac output variations larger than 1% were also corrected for. The threshold feature of the software was set so as to include dose ranging from 20% to 500% in the gamma calculation, with doses normalized to the isocenter dose. Because the system design includes a diode located at isocenter, the software was used to compare the dose measured at isocenter to the TPS's prediction of dose at the same position.

2.6. Validation of arc-based measurement systems (Delta4)

Because the Delta4 device is a relatively new system that is specially designed to validate arc-based deliveries, we believed it prudent to validate the accuracy of dose measurements obtained using this new system with a more 'conventional' film and ion chamber validation. The validation methodology we used was to validate the Delta4 system for 12 redundant sample

plans. The film phantom consisted of two blocks of water-equivalent material between which a coronally oriented sheet of EDR2 film (Eastman-Kodak, Rochester, NY, USA) was inserted for planar dose measurement. One of the blocks also had a hole designed to accept a 0.3 cc PTW N31013 (PTW, Freiburg, Germany) ion chamber for an absolute dose measurement at a centrally located point, slightly below the coronal plane of the film. Because film saturates at high doses, two plans were created in cases where the expected dose to the film exceeded 3 Gy. One was for the full dose and was used to measure time of delivery and ion chamber point dose. The second plan was developed with a scaled-down level of dose, and both ion chamber and film measurements were obtained. The ion chamber reading was corrected for temperature and pressure effects at the time of delivery and for linac output variations larger than 1%.

After the film was processed, it was scanned with a Vidar film scanner (model VXR-16, Vidar Systems Corp, Herndon, VA, USA) and the image was transferred to the RIT113 software (version 5.2, Radiological Imaging Technology, Colorado Springs, CO, USA) for dose evaluation. The film was calibrated using a calibration curve previously developed for the same linac and the measured dose plane was compared to the calculated dose plane exported from Prowess. Films were normalized to the maximum dose and all points with 20% or greater dose were included in the gamma analysis. We used vertical and horizontal profiles to visually compare the film dose distribution to the Delta4 distribution and we used the gamma index (3 mm/3%) to quantitatively compare the film and Delta4 distributions.

3. Results

With all relevant software and hardware interlocks intact, the converted Artiste linac was confirmed to be capable of delivering all treatment plans in the experimental mode, without machine fault or other undesired delivery anomaly. Table 2 shows the results of the 21 dose validations performed using the Delta4 measurement device on the arc plans developed for the seven treatment sites described in table 1. Arc plans can be seen to agree with prediction at the central axis to within 3% or better (mean $= -0.1\%$, Max $= 2.9\%$) and the proportion of measurements with gamma (3%, 3 mm) index less than unity was above 90% (mean $=$ 98.5%; Min $= 94.6\%$). The data further show that the linac is capable of delivering the more complex burst mode modulated arc treatments with dose accuracy that is comparable to both of the simpler, unmodulated conformal arc and segment weighted conformal arc delivery approaches.

Table 3 shows relevant dosimetric metrics from the plans created, while figure 4 shows isodose distributions from three representative sites showing how plan quality compared.

Table 4 shows the results of film/ion chamber validation tests performed to confirm the accuracy of the results measured using the Delta4 system. The ion chamber measurements, relative to TPS prediction, were compared to the central axis dose measured by the Delta4 measurement device, relative to TPS prediction, and all were found to agree with their respective TPS prediction to within 3%, thus confirming that dose validation with the Delta4 at isocenter yields similar results to ion chamber in solid water at isocenter. Also included in the table are the results of the gamma analysis performed on the film dose distribution, and compared to the results obtained in the Delta4 system. Gamma pass rates for film and Delta4, relative to their respective TPS predictions, are seen to be in good agreement with each other, thus indicating reliability of the Delta4 gamma pass rate results.

Table 5 lists the treatment plan delivery time measurements for all plans. It is apparent that, in general, arc methods of delivery require roughly half of the delivery time compared to the

Table 3. Relevant dosimetric metrics from the different plans compared. Cases where an evaluation criterion was violated are in bold.

Site	Metric	Evaluation No violation	Criteria Minor violation	Modality CA	SWCA	MA	SG-IMRT	3DCRT
Cavernous sinus	PTV V100% (%)	⩾95%	–	95.1	95.1	97.4	97.1	95.1
	PTV V95% (%)	⩾ 99%	–	99.6	99.4	99.2	99	99
	Brainstem Max (Gy)	<12 Gy	–	**13.9**	**13**	11.4	10.5	11.9
Lung	PTV D95% (Gy)	⩾60Gy	–	60	60	60	60	60.2
	PTV D99% (Gy)	⩾54Gy	–	57.4	57.6	55.8	58.9	57.3
	Spine Max (Gy)	<18 Gy	18–18.9 Gy	10.4	11.6	17.6	14.6	6.6
	Heart Max (Gy)	<24 Gy	24–25.2 Gy	13.7	23.4	23.3	17.3	13.7
	Lung V20 Gy (%)	<10%	10–15%	**11.6**	9.7	**11.4**	7	6.6
Prostate (1.8 Gy)	PTV D98% (Gy)	⩾73.8		73.9	73.8	73.8	73.9	73.8
	PTV Max (Gy)	<79	> = 79, < = 81.2	**83.5**	81.1	78.3	78.5	81.2
	Bladder V65 Gy (%)	<50%	–	5.9	8.1	7.8	9	14.6
	Rectum V60 Gy (%)	<50%	–	11.5	12.8	11.8	12.5	20.3
	Penile Bulb Mean (Gy)	<52.5 Gy	–	29.9	29.5	34.1	32.3	21.1
Prostate (2.5 Gy)	PTV D98% (Gy)	⩾70	–	70.1	70	70.1	70	70
	PTV Max (Gy)	⩽74.9	>74.9, < = 77	**79.2**	77	74.1	74.9	77
	Bladder V65 Gy (%)	<50%	–	5	7.1	7.1	8.8	12.6
	Rectum V60 Gy (%)	<50%	–	10.3	11.9	9.3	15.4	19.3
	Penile Bulb Mean (Gy)	⩽51 Gy	–	28.3	33.8	27.9	33	20
Liver	PTV D90% (%)	–	–	99.4	99.8	99.7	100	100
	Cord Max (Gy)	–	–	1.4	0.8	0.9	0.4	1.6
	Rt. Kidney Max (Gy)	–	–	2.5	2.1	2.3	2.3	5.9
	Lt. Kidney Max (Gy)	–	–	0.6	0.9	1.2	1.6	1.5
Spine RPC phantom	PTV D90% (Gy)	⩾6Gy	–	6	6	6	6	6
	Spine Max (Gy)	⩽5.25 Gy	–	**6.6**	**5.8**	3.5	3.1	1.8
	Heart Max (Gy)	⩽8.25 Gy	–	1.8	0.8	1.3	2.9	0.1
	Esophagus Max (Gy)	⩽6Gy	–	3.8	2	3.3	2.7	0.8
H&N RPC phantom	PTV1 V6.6 Gy (%)	⩾95%	–	95.6	95.4	96	95.2	97.2
	PTV2 V5.4 Gy (%)	⩾95%	–	95.1	99.8	97.3	100	97.6
	OAR Max (Gy)	⩽4.5 Gy	–	**7.3**	**7**	4.4	4.2	4.5

corresponding static-gantry IMRT plan. As would be expected, segment-weighted conformal arcs generally take slightly longer than conformal arcs (mean = 2.9%), and modulated arcs generally take slightly longer than segment-weighted conformal arcs (mean = 35.9%). Of course, the more complex MA delivery approach typically outperforms the CA and SWCA approaches on challenging plans. For example, the CA and SWCA plans experienced 16 violations of planning requirements across all plans, while the MA plans experienced only one minor violation (see table 3).

4. Discussion

A new burst mode delivery approach for modulated arc treatment has been described and evaluated here. In order to verify feasibility of use in the clinical environment, the delivery

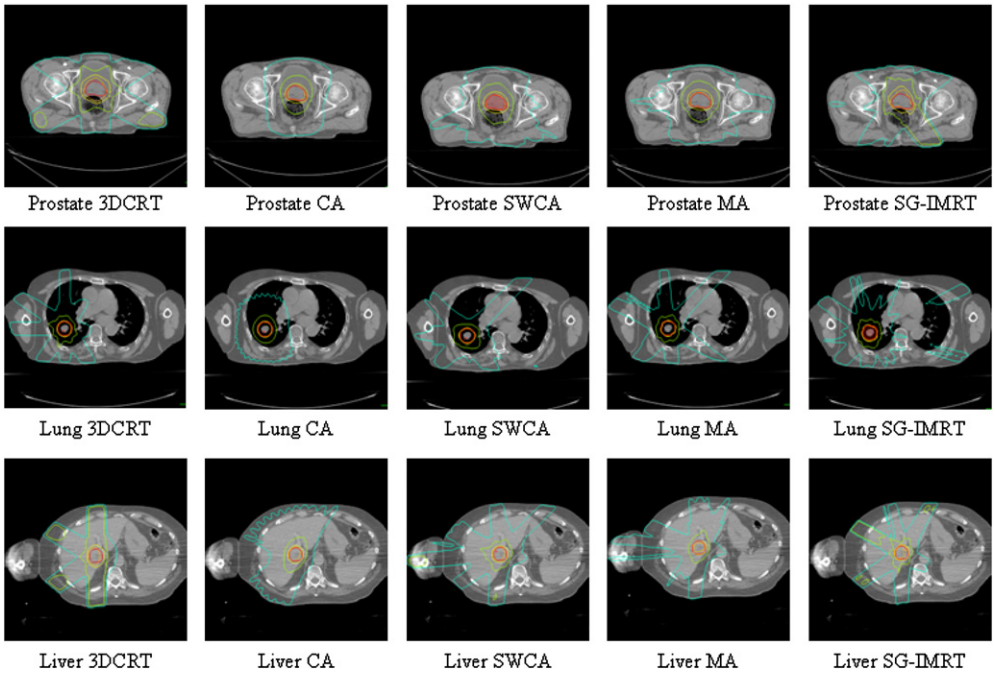

Figure 4. Isodose distributions from the same CT slice for the prostate (2.5 Gy per fraction), lung and liver cases. The PTV is shown in red. The orange isodose distribution shows the prescription line (70 Gy for prostate, 60 Gy for lung and 36 Gy for liver); the yellow, green and blue lines show the 90%, 50% and 20% prescription isodose, respectively.

approach was evaluated for delivery of treatments at numerous clinical sites, using clinically relevant treatment design criteria, and all treatments explored here were seen to deliver without machine fault or anomaly.

The burst mode delivery approach was seen to closely approach the approximation that treatment planning systems use to calculate dose, namely as a summation of statically delivered fields. As such, the method should contribute to high accuracy of delivered dose and, indeed, this is what we observed when validating the accuracy of dose delivery across an array of clinically relevant treatment sites. When validated by either Delta4 volumetric phantom or film and ion chamber in solid water, delivered dose was confirmed to agree quite well with the dose predicted by the prototype Prowess TPS.

A primary source of recent interest in modulated arc-based treatment approaches has been the desire to achieve the benchmark plan 'quality' of complex and time consuming many-field static-gantry IMRT approaches, but with much reduced treatment delivery time. For purposes of characterizing the efficiency of delivery of the burst mode modulated arc prototype system evaluated here, we developed and timed delivery of static-gantry treatment plans for multiple, clinically relevant treatment sites. The burst mode delivery approach resulted in treatment times that required, on average, 38% less time to deliver than the equivalent static-gantry IMRT approach, while satisfying all dosimetric planning requirements, with far fewer minor protocol violations compared to the simpler conformal techniques.

Table 4. Comparison between validation results obtained using the Delta4 system and the corresponding results obtained using film and ion-chamber measurements. The purpose is to confirm that validations performed using the Delta4 device are consistent with results obtained from the more familiar film with ion chamber in solid water approach. A subset of sites was selected for this study and the data show that Delta4 validation results were comparable to film with ion chamber results.

Site	Modality	Rx dose (Gy)	Measured dose difference from expected (%)	Gamma pass rate (3%, 3 mm)	Measured with
		1.5	−0.8%	99.3%	Film/ion chamber
Lung	CA	20.0	1.5%	N/A	Ion chamber
		20.0	1.4%	100%	Delta4
		1.5	−0.4%	99.8%	Film/ion chamber
Lung	SWCA	20.0	1.0%	N/A	Ion chamber
		20.0	1.2%	99.3%	Delta4
		1.5	1.3%	98.9%	Film/ion chamber
Lung	MA	20.0	1.7%	N/A	Ion chamber
		20.0	1.3%	97.1%	Delta4
Prostate	CA	1.8	1.0%	95.3%	Film/ion chamber
		1.8	0.5%	100%	Delta4
Prostate	SWCA	1.8	2.6%	97.9%	Film/ion chamber
		1.8	−1.6%	100%	Delta4
Prostate	MA	1.8	2.3%	99.7%	Film/ion chamber
		1.8	0.0%	100%	Delta4
		1.5	2.6%	99.8%	Film/ion chamber
Prostate	CA	2.5	2.7%	N/A	Ion chamber
		2.5	0.4%	100%	Delta4
		1.5	2.8%	98.5%	Film/ion chamber
Prostate	SWCA	2.5	2.3%	N/A	Ion chamber
		2.5	−1.1%	100%	Delta4
		1.5	2.2%	99.8%	Film/ion chamber
Prostate	MA	2.5	2.6%	N/A	Ion chamber
		2.5	−0.4%	100%	Delta4
		1.5	2.3%	97.9%	Film/ion chamber
Liver	CA	12.0	1.1%	N/A	Ion chamber
		12.0	0.6%	97.3%	Delta4
		1.5	2.5%	98.2%	Film/ion chamber
Liver	SWCA	12.0	1.2%	N/A	Ion chamber
		12.0	0.5%	97.8%	Delta4
		1.5	2.2%	98.5%	Film/ion chamber
Liver	MA	12.0	0.3%	N/A	Ion chamber
		12.0	0.6%	95.1%	Delta4

Table 5. A comparison of the delivery times for the plans created for the different sites investigated in this work. The delivery times for arc plans are compared to a static gantry IMRT (SG-IMRT) and 3D conformal (3DCRT) plan developed using the same planning criteria as the arc plans.

Site	Modality	Rx dose (Gy)	Delivery time
	CA	15.0	2 min 51 s
	SWCA	15.0	2 min 59 s
Cavernous sinus	MA	15.0	4 min 17 s
	SG-IMRT	15.0	8 min 37 s
	3D-CRT	15.0	3 min 52 s
	CA	20.0	3 min 25 s
	SWCA	20.0	3 min 20 s
Lung	MA	20.0	4 min 42 s
	SG-IMRT	20.0	9 min 46 s
	3D-CRT	20.0	3 min 55 s
	CA	1.8	2 min 08 s
	SWCA	1.8	1 min 56 s
Prostate	MA	1.8	2 min 35 s
	SG-IMRT	1.8	4 min 10 s
	3D-CRT	1.8	2 min 11 s
	CA	2.5	1 min 45 s
	SWCA	2.5	1 min 55 s
Prostate	MA	2.5	2 min 31 s
	SG-IMRT	2.5	4 min 20 s
	3D-CRT	2.5	2 min 19 s
	CA	12.0	2 min 06 s
	SWCA	12.0	2 min 12 s
Liver	MA	12.0	3 min 09 s
	SG-IMRT	12.0	4 min 57 s
	3D-CRT	12.0	2 min 20 s
	CA	6.0	1 min 48 s
	SWCA	6.0	2 min 05 s
Spine RPC phantom	MA	6.0	3 min 10 s
	SG-IMRT	6.0	6 min 49 s
	3D-CRT	6.0	1 min 16 s
	CA	6.6	2 min 31 s
	SWCA	6.6	2 min 18 s
H&N RPC phantom	MA	6.6	3 min 15 s
	SG-IMRT	6.6	9 min 17 s
	3D-CRT	6.6	3 min 09 s

5. Conclusions

Burst mode modulated arc delivery, wherein 2000 MU min^{-1} high dose rate bursts of dose were facilitated by a flattening-filter-free prototype treatment beam, was implemented, described

and tested. The Artiste linac, enabled for burst mode, was confirmed to be capable of delivering a wide array of clinically relevant treatment plans, without machine fault or other undesired delivery anomaly. The method was seen to yield treatment delivery that closely approaches the static field methodology by which modern treatment planning systems approximate arc-based deliveries for calculation. Dosimetric accuracy of the Artiste burst mode prototype delivery platform, as well as the Prowess prototype treatment planning version utilized here, were confirmed to be excellent. The modulated arc treatment system evaluated here appears to represent a capable and efficient delivery approach and is the subject of ongoing collaborative investigations by our research group.

Acknowledgments

We wish to acknowledge grant support for this research by Siemens, and also to express appreciation for guidance and support from the Siemens team in Concord, CA, USA. In particular, we express our thanks to Ali Bani-Hasheni, Paco Hernandez, Johannes Stahl, Marcelo Cassese and Chris Amies for support and insight. We also wish to thank the team at Prowess Medical for invaluable support with the prototype treatment planning system utilized for burst mode calculations and the ScandiDOS Company for providing their Delta4 arc validation hardware. Finally, our gratitude goes to our local linear accelerator engineer, Harry English, for his after-hours support of measurement acquisition.

References

Bayouth J E 2008 Siemens multileaf collimator characterization and quality assurance approaches for intensity-modulated radiotherapy *Int. J. Radiat. Oncol. Biol. Phys.* **71** S93–7

Bayouth J E, Kaiser H S, Smith M C, Pennington E C, Anderson K M, Ryken T C and Buatti J M 2007 Image-guided stereotactic radiosurgery using a specially designed high-dose-rate linac *Med. Dosim.* **32** 134–41

Bedford J L 2009 Treatment planning for volumetric modulated arc therapy *Med. Phys.* **36** 5128–38

Bedford J L, Lee Y K, Wai P, South C P and Warrington A P 2009 Evaluation of the Delta4 phantom for IMRT and VMAT verification *Phys. Med. Biol.* **54** N167–76

Bedford J L and Warrington A P 2009 Commissioning of volumetric modulated arc therapy (VMAT) *Int. J. Radiat. Oncol. Biol. Phys.* **73** 537–45

Feygelman V, Zhang G and Stevens C 2010 Initial dosimetric evaluation of SmartArc—a novel VMAT treatment planning module implemented in a multi-vendor delivery chain *J. Appl. Clin. Med. Phys.* **11** 99–116

Haga A *et al* 2009 Quality assurance of volumetric modulated arc therapy using Elekta Synergy *Acta Oncol.* **48** 1193–7

Kirkpatrick S, Gelatt C D Jr and Vecchi M P 1983 Optimization by simulated annealing *Science* **220** 671–80

Kjaer-Kristoffersen F, Ohlhues L, Medin J and Korreman S 2009 RapidArc volumetric modulated therapy planning for prostate cancer patients *Acta Oncol.* **48** 227–32

Li X A, Ma L, Naqvi S, Shih R and Yu C 2001 Monte Carlo dose verification for intensity-modulated arc therapy *Phys. Med. Biol.* **46** 2269–82

Ling C C, Zhang P, Archambault Y, Bocanek J, Tang G and Losasso T 2008 Commissioning and quality assurance of RapidArc radiotherapy delivery system *Int. J. Radiat. Oncol. Biol. Phys.* **72** 575–81

Mayo C S, Ding L, Addesa A, Kadish S, Fitzgerald T J and Moser R 2009 Initial experience with volumetric IMRT (RapidArc) for intracranial stereotactic radiosurgery *Int. J. Radiat. Oncol. Biol. Phys.* **78** 1457–66

Otto K 2008 Volumetric modulated arc therapy: IMRT in a single gantry arc *Med. Phys.* **35** 310–7

Ponisch F, Titt U, Vassiliev O N, Kry S F and Mohan R 2006 Properties of unflattened photon beams shaped by a multileaf collimator *Med. Phys.* **33** 1738–46

Stathakis S, Esquivel C, Gutierrez A, Buckey C R and Papanikolaou N 2009 Treatment planning and delivery of IMRT using 6 and 18 MV photon beams without flattening filter *Appl. Radiat. Isot.* **67** 1629–37

Tacke M B, Nill S, Haring P and Oelfke U 2008 6 MV dosimetric characterization of the 160 MLC, the new Siemens multileaf collimator *Med. Phys.* **35** 1634–42

Yoda K, Nakagawa K, Shiraishi K, Okano Y, Ohtomo K and Pellegrini R G 2009 Dose verification of intensity-modulated arc therapy using an ERGO++ treatment planning system and Elekta internal multileaf collimators for prostate cancer treatment *Br. J. Radiol.* **82** 328–31

Yu C X 1995 Intensity-modulated arc therapy with dynamic multileaf collimation: an alternative to tomotherapy *Phys. Med. Biol.* **40** 1435–49

Zacarias A S, Brown M F and Mills M D 2009 Volumetric modulated arc therapy (VMAT) treatment planning for superficial tumors *Med. Dosim.* **35** 226–9